# Mobile Acoustic Communications: Real Data Analysis of Partial FFT Demodulation with Coherent Detection

Munish Taya, Amir Tadayon and Milica Stojanovic
Northeastern University, Boston, MA, USA

***Abstract*—We address the use of orthogonal frequency division multiplexing (OFDM) for high-rate communication over a mobile acoustic channel. To counteract the frequency offset and time-variability of the broadband mobile channel, we employ a dedicated method for synchronization and partial FFT (P-FFT) demodulation, cast into the framework of multichannel diversity combining. Unlike conventional receivers, where the signal is demodulated using a single FFT operating over the full OFDM block interval, P-FFT employs multiple FFT operations to demodulate the signal over several partial intervals. The partial demodulator outputs are subsequently combined, and the combined signal is fed to a second stage, where refined channel estimation and data detection take place. We investigate both coherent and differentially coherent detection, and test refined channel estimation with least squares (LS) and matching pursuit (MP) algorithms. Partial interval demodulation offers an additional degree of freedom by allowing for suppression of time-variation before inter-carrier interference has been created in the process of demodulation. The result is an improved quality of data detection, which we demonstrate using real data recorded during the 2010 Mobile Acoustic Communications Experiment MACE'10. Results of experimental data processing show excellent performance with up to 2048 QPSK-modulated carriers operating in the 10.5 kHz - 15.5 kHz acoustic band over varying distance (3-7 km) and speeds up to 1.5 m/s.**

## I. Introduction

Orthogonal frequency division multiplexing (OFDM) offers an efficient way of equalizing a frequency-selective channel, and has for this reason been considered for achieving high-rate underwater acoustic communications [1]. In situations with high mobility, however, OFDM is challenged by the time-variability of the channel, as the Doppler effect causes carrier frequencies to shift, thus creating inter-carrier interference (ICI) which has a detrimental impact on data detection performance [2]–[6].

Over the recent years, many studies have investigated the issue of ICI mitigation, conventionally focusing on post-FFT signal processing. The authors in [7] proposed a progressive receiver based on the turbo principle which begins as an ICI ignorant receiver and iteratively increases the span of ICI on the post-FFT signal until the block is decoded successfully. Ref. [3] proposed an explicit and implicit method for mitigating ICI. In the explicit method, it is assumed that ICI affects a pre-specified set of adjacent carriers, and is mitigated by estimating the ICI coefficients based on a closed-loop approach. In contrast, the implicit method does not rely on ICI coefficient estimation, but instead employs an adaptive decision feedback equalizer in the frequency domain across adjacent carriers.

Unlike conventional methods, the authors in [5] proposed a method called partial FFT demodulation (P-FFT), which targets pre-FFT signal processing to counteract the channel's time-variation *before* ICI has been created in the process of demodulation. To do so, the time interval of one OFDM block is divided into several partial intervals, giving the channel less chance to change over each shorter interval, and demodulation is performed in each interval separately. The partial demodulator outputs are then combined in a weighted sum, thus compensating for the channel variation within a block. The pre-combined signals are finally processed by a second stage, consisting of standard least squares (LS) channel estimation and subsequent data detection.

Estimating the acoustic channel puts an overhead of pilots, and this motivated the authors in [6] to use differentially coherent detection with P-FFT demodulation. Differentially coherent detection eliminates the need for channel estimation relying instead on the assumption that the channel response changes slowly across the carriers. Operating under a least mean squares (LMS) algorithm for computing the P-FFT combiner coefficients, the method was successfully demonstrated on real data.

In this paper, we re-visit P-FFT demodulation with coherent detection, following the general approach of [5]. However, while [5] used simulation to show that P-FFT offers a viable way of restoring the OFDM performance on a highly time-varying channel, we report here on the results of processing real data recorded during the 2010 Mobile Acoustic Communications Experiment (MACE'10). To make the method suitable for practical acoustic channels, we introduce several features: (1) we replace the LS channel estimation of [5] by the super-resolution matching pursuit (MP) algorithm [8] which offers an advantage in estimating the naturally sparse acoustic channels, and (2) we cast the receiver processing into multichannel framework to exploit the spatial diversity through maximum ratio combining (MRC). We also report on the results of applying differentially coherent P-FFT combining to real data, for which we follow the general approach of [6], but use a method based on recursive least square (RLS) computation to replace the LMS, thus aiming for faster convergence.

978-1-5386-4814-8/18/$31.00 ©2018 IEEE

The results of experimental data processing show excellent performance with up to 2048 QPSK-modulated carriers operating in the 10.5 kHz - 15.5 kHz acoustic band over varying distance (3-7 km) and speeds up to 1.5 m/s. Partial FFT demodulation demonstrates remarkable performance, with both coherent and differentially coherent detection. Coherent detection outperforms differentially coherent detection at the expense of computational complexity needed for channel estimation. Using super-resolution MP for channel estimation offers a further improvement over the standard LS, reaching an impressive performance in conditions of high mobility.

The rest of the paper is organized as follows. Sec. II provides a brief description of the OFDM system with P-FFT demodulation. Sec. III details the receiver algorithm for coherent and differentially coherent detection. Sec. IV contains the results of experimental data processing. We conclude in Sec. V.

## II. System Model

We consider an OFDM system with $M_r$ receiving elements and $K$ carriers operating in bandwidth $B$. The signal transmitted during one OFDM block is

$$s(t) = Re\left\{\sum_{k=0}^{K-1} d_k e^{j2\pi f_k t}\right\}, \quad t \in [0,T] \tag{1}$$

where $T = 1/\Delta f$ is the block duration, $\Delta f = B/K$ is the carrier spacing, $f_k = f_0 + k\Delta f$ is the $k$th carrier frequency, and $d_k$ is the unit-amplitude PSK symbol transmitted on the $k$th carrier. The signal received on the $m$th receiving element is modeled as [9]

$$r^m(t) = \sum_p h_p^m(t) s(t-\tau_p^m(t)) + n^m(t),\ m = 1,\dots,M_r \tag{2}$$

where $h_p^m(t)$ and $\tau_p^m(t)$ represent the $p$-th path gain and delay, respectively. The noises $n^m(t)$ are assumed to be zero-mean and independent across receiving elements. After frame synchronization, initial resampling, downshifting by the lowest carrier frequency and cyclic prefix removal, the received signal on $m$th receiver is given by

$$v^m(t) = \sum_{k=0}^{K-1} d_k H_k^m(t) e^{j2\pi k\Delta f t} + w^m(t),\ t \in [0,T] \tag{3}$$

where $H_k^m(t) = \sum_p h_p^m(t) e^{-j2\pi f_k \tau_p^m(t)}$ is the time-varying frequency response of the channel on the $k$th carrier of the $m$th receiving element, and $w^m(t)$ is the equivalent baseband noise.

Partial FFT demodulation with $I$ intervals yields the observations

$$y_{k,i}^m = \frac{1}{T}\int_{iT/I}^{(i+1)T/I} v^m(t) e^{-j2\pi k\Delta f t} dt,\ i = 0,\dots I-1 \tag{4}$$

In practice, the same observations can be obtained by applying an FFT operation to the input $v^m(t)\phi_i(t)$, where $\phi_i(t),\ i = 0,\dots,I-1$ are the unit-amplitude rectangular pulses which divide the OFDM block into $I$ non-overlapping sections. If the duration of each section is short enough, the corresponding channel variation can be considered negligible [5], [6]. Fig. 1 represents the block diagram of P-FFT demodulation with $I = 4$ FFT blocks.

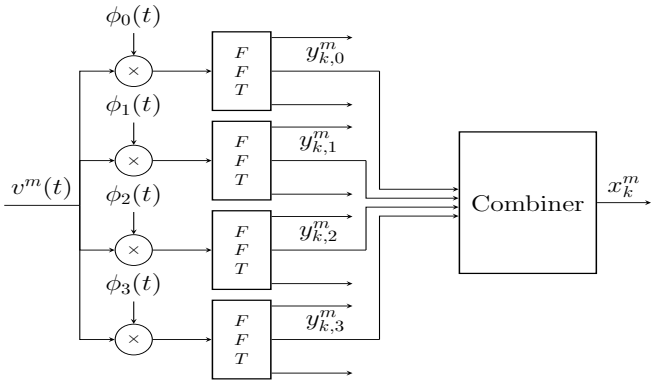


Fig. 1: Partial FFT demodulation with $I = 4$ intervals captured by functions $\phi_i(t),\ i = 0,\dots,I-1$. Weighted combining aims for suppression of ICI.

## III. Receiver Algorithms

### A. Coherent P-FFT combining

The observations obtained from P-FFT demodulators are linearly combined to produce the signals

$$x_k^m = \sum_i p_{k,i}^{m*} y_{k,i}^m = \mathbf{p}_k^{m'} \mathbf{y}_k^m \tag{5}$$

where $\mathbf{p}_k^m$ is the column vector of P-FFT combiner coefficients, and $\mathbf{y}_k^m$ is the corresponding vector of demodulator outputs.[1] Assuming that the signals $x_k^m$ contain no ICI, these signals are modeled as

$$x_k^m = H_k^m d_k + z_k^m \tag{6}$$

where $H_k^m$ is the equivalent post-combining channel coefficient (not to be confused with $H_k^m(t)$), and $z_k^m$ is the corresponding noise.

Assuming that the channel estimate $\hat{H}_k^m$ is available, the data symbol estimates are formed through MRC as

$$\hat{d}_k = \frac{\sum_m \hat{H}_k^{m*} x_k^m}{\sum_m |\hat{H}_k^m|^2} \tag{7}$$

and the decisions $\tilde{d}_k$ are made on the so-obtained estimates. The MRC coefficients $\hat{H}_k^m$ and the P-FFT combiner vectors $\mathbf{p}_k^m$ can now be computed recursively over the carriers. The updated vectors $\mathbf{p}_{k+1}^m$ are computed by applying the RLS algorithm to the current values $\mathbf{p}_k^m$, the input $\mathbf{y}_k^m$ and the error $\epsilon_k^m = x_k^m - \hat{H}_k^m \tilde{d}_k$, where $\tilde{d}_k = d_k$ for $k$ in the pilot

[1] Prime and $()^*$ stand for conjugate transpose and complex conjugate, respectively.

set $\mathcal{K}_p$, or the decision made on the estimate. The equivalent channel estimate is computed as

$$\hat{H}_{k+1}^m = \alpha \hat{H}_k^m + (1-\alpha)\frac{x_k^m}{\tilde{d}_k} \tag{8}$$

where $\alpha \in [0,1)$, accounts for smoothing. The algorithm is summarized in the Algorithm 1 table.

P-FFT combiner weights are initialized as a vector of all ones, and the first $2I$ carriers are designated as pilots for initial convergence. The algorithm is then switched into decision directed mode. To guard against error propagation in decision-directed mode, additional pilots are inserted periodically throughout the OFDM block.

### *B. Refinement*

The above expressions define the first stage of processing, in which coherent combining of the partial FFT outputs is performed. Once the first stage is completed, the signals $x_k^m$ and the tentative decisions $\tilde{d}_k$, acting as pilots, are fed to a second stage, where a refined channel estimate is formed using the MP algorithm [8]. Algorithm steps corresponding to the MP refinement are also listed in the Algorithm 1 table. In this implementation, we use the super-resolution MP algorithm, in which the impulse response is discretized in steps of $T/SK$, where $S \geq 1$ is a positive integer that accounts for increased resolution in the delay domain. Using a resolution higher than the basic $T/K$ reduces the power spillage among adjacent taps of the estimated impulse response, ultimately aiming for a minimal channel representation where the number of taps equals the number of physical propagation paths [2]. The algorithm terminates when the absolute ratio of the estimated tap to the strongest tap falls below a pre-specified threshold $\eta$.

### *C. Differentially coherent P-FFT combining*

Differentially coherent detection capitalizes on the coherence between adjacent carriers to eliminate the need for channel estimation. In light of partial FFT combining, coherence in the frequency domain is expressed by the fact that $H_{k-1}^m \approx H_k^m$. To take advantage of this condition, data symbols are differentially encoded prior to transmission. Specifically, if we denote by $b_k$ the original data symbol stream, differential encoding yields the transmitted stream $d_k = b_k d_{k-1}$.[2]

Based on the assumption (6), differential maximum ratio combining (DMRC) yields the data symbol estimates

$$\hat{b}_k = \frac{\sum_m x_{k-1}^{m*} x_k^m}{\sum_m |x_{k-1}^m|^2} = \frac{\mathbf{x}'_{k-1}\mathbf{x}_k}{\mathbf{x}'_{k-1}\mathbf{x}_{k-1}} \equiv \bar{\mathbf{x}}'_{k-1}\mathbf{x}_k \tag{9}$$

where $\mathbf{x}_k = \begin{bmatrix} x_k^1 & x_k^2 & \dots & x_k^{M_r} \end{bmatrix}^T$ is the vector of P-FFT demodulator outputs (5), and $\bar{\mathbf{x}}_k = \mathbf{x}_k/||\mathbf{x}_k||^2$. Final decision $\tilde{b}_k$ is made on the estimates $\hat{b}_k$.

To compute the P-FFT combiner coefficients, we again employ the RLS algorithm. Grouping all the P-FFT combiner vectors into a single column vector $\mathbf{p}_k$ with constituent

[2]The encoding process conventionally begins with $d_0 = 1$, which is known to both the transmitter and the receiver.

**Algorithm 1** Coherent P-FFT Demodulation with MP

INITIALIZATION:

- Initialize combining weight vectors $\mathbf{p}_0^m = \mathbf{1}_{I\times 1} = [1, \cdots, 1]^T,\ \forall m = 1, \dots, M_r$.
- Initialize channel estimate vector $\hat{H}_0^m = 1,\ \forall m = 1, \dots, M_r$.
- Pilot set $\mathcal{K}_p$.
- Inverse covariance matrix $\mathbf{Q}_0^m = 10^3\mathbf{I},\ \forall m = 1, \dots, M_r$; $\mathbf{I}$ is an identity matrix of size $I \times I$.
- $\mathbf{F}$: first $K$ rows of DFT matrix of size $SK$.
- $\mathbf{f}_l$ : $l$th column of $\mathbf{F}$.
- Termination threshold $\eta$.

COHERENT P-FFT DEMODULATION:

**for** $k \leftarrow 0, K-1$ **do**
  **for** $m \leftarrow 1, M_r$ **do**
    $x_k^m = \mathbf{p}_k^{m\prime}\mathbf{y}_k^m$
  **end for**
  $\hat{d}_k = \frac{\sum_m \hat{H}_k^{m*} x_k^m}{\sum_m |\hat{H}_k^m|^2}$
  **if** $k \in \mathcal{K}_p$ **then**
    $\tilde{d}_k = d_k$
  **else**
    $\tilde{d}_k = dec\{\hat{d}_k\}$
  **end if**
  **for** $m \leftarrow 1, M_r$ **do**
    $\epsilon_k^m = \tilde{d}_k \hat{H}_k^m - x_k^m$
    $\mathbf{g}_k^m = \frac{\mathbf{Q}_k^m \mathbf{y}_k^m}{\lambda + \mathbf{y}_k^{m\prime}\mathbf{Q}_k^m\mathbf{y}_k^m}$
    $\mathbf{Q}_{k+1}^m = \frac{\mathbf{Q}_k^m - \mathbf{g}_k^m \mathbf{y}_k^{m\prime}\mathbf{Q}_k^m}{\lambda}$
    $\mathbf{p}_{k+1}^m = \mathbf{p}_k^m + \mathbf{g}_k^m \epsilon_k^{m*}$
    $\hat{H}_{k+1}^m = \alpha\hat{H}_k^m + (1-\alpha)\frac{x_k^m}{\tilde{d}_k}$
  **end for**
**end for**

MATCHING PURSUIT REFINEMENT:

**for** $m \leftarrow 1, M_r$ **do**
  $\hat{\mathbf{b}}^m = 0_{SK\times 1}$
  $J = \{\}$
  $\mathbf{r}^m = \mathbf{x}^m = \begin{bmatrix} x_0^m & \cdots & x_{K-1}^m \end{bmatrix}^T$
  **repeat**
    $l = \arg\max_{j \notin J_{k-1}} |\mathbf{f}_j'\mathbf{r}^m|$
    $J = J \cup \{l\}$
    $\hat{b}_l^m = \frac{1}{K}\mathbf{f}_l'\mathbf{r}^m$
    $\mathbf{r}^m = \mathbf{r}^m - \hat{b}_l^m \mathbf{f}_l$
  **until** $10\log_{10}|\frac{\hat{b}_l^m}{(\max_{j\in J}\ \hat{b}_j^m)}| > \eta$
  $\widehat{\mathbf{H}}^m = \begin{bmatrix} \hat{H}_0^m & \cdots & \hat{H}_{K-1}^m \end{bmatrix}^T = \mathbf{F}\hat{\mathbf{b}}^m$
**end for**

DATA DETECTION:

**for** $k \leftarrow 0, K-1$ **do**
  $\hat{d}_k = \frac{\sum_m \widehat{H}_k^{m*} x_k^m}{\sum_m |\widehat{H}_k^m|^2}$
**end for**

| Number of carriers, $K$ | 128 | 256 | 512 | 1024 | 2048 |
|---|---|---|---|---|---|
| number of blocks per frame, $N_b$ | 64 | 32 | 16 | 8 | 4 |
| carrier spacing, $\Delta f$ [Hz] | 39.1 | 19.5 | 9.8 | 4.9 | 2.4 |
| block duration, $T$ [ms] | 26.2 | 52.4 | 105 | 210 | 419 |
| bit rate, $R_b$ [kbps] (coherent) | 4.71 | 6.25 | 7.33 | 7.99 | 8.36 |
| bit rate, $R_b$ [kbps] (differential) | * | 1.90 | 5.41 | 7.54 | 8.72 |
| bandwidth efficiency [bps/Hz] (coherent) | 0.94 | 1.25 | 1.47 | 1.60 | 1.67 |
| bandwidth efficiency [bps/Hz] (differential) | * | 0.38 | 1.08 | 1.51 | 1.74 |

TABLE I: OFDM signal parameters used in the MACE'10 experiment. Total bandwidth is $B = 5$ kHz and the lowest carrier frequency is $f_0 = 10.5$ kHz. The effective symbol rate is $R = (K - |\mathcal{K}_p|)/(T + T_g)$, where $T_g = 16$ ms is the guard interval between consecutive OFDM blocks of duration $T = K/B$, and $|\mathcal{K}_p|$ is the number of pilots computed for $I = 8$ partial intervals and $M_r = 12$ receiving elements. With $K = 128$ carriers, there are insufficiently many pilots for differentially coherent combining; this case is marked by the asterisks. QPSK modulation is used, yielding a bit rate $R_b = 2R$.

components $\mathbf{p}_k^1, \dots \mathbf{p}_k^{M_r}$, the data symbol estimate (9) can be expressed as

$$\hat{b}_k = \mathbf{p}_k' \mathbf{u}_k \tag{10}$$

where the column vector $\mathbf{u}_k$ has constituent components

$$\mathbf{u}_k^m = \bar{x}_k^{m*} \mathbf{y}_k^m, \ m = 1, \dots M_r \tag{11}$$

With the dependence of $\hat{b}_k$ on $\mathbf{p}_k$ now explicitly stated by the expression (10), the RLS algorithm computes $\mathbf{p}_{k+1}$ based on the current value $\mathbf{p}_k$, the input $\mathbf{u}_k$ and the error $e_k = \hat{b}_k - \tilde{b}_k$, where $\tilde{b}_k$ is either a known symbol from the pilot set, or a decision made on $\hat{b}_k$. With the RLS algorithm the number of pilots $|\mathcal{K}_p|$ needed to ensure convergence is about twice the size of the vector $\mathbf{p}_k$ i.e., $2IM_r$. Note that this number of pilots is greater than for coherent detection because DMRC is performed jointly over all the partial vectors $\mathbf{p}_k^m$.

## IV. Experimental Results

Signals recorded during the MACE'10 experiment were used to analyze the performance of the P-FFT demodulation algorithms. The experiment was conducted off the coast of Martha's Vineyard, Massachusetts, in June 2010. Signals were transmitted in the acoustic frequency range between 10.5 kHz and 15.5 kHz, in a total of 52 rounds. Each round was repeated every 4 minutes for a total duration of 3.5 hours, as the transmitter moved towards and away from the receiver at varying speeds ranging from 0.5 m/s to 1.5 m/s. Each round included the transmissions of all the OFDM signals, whose parameters are listed in Table I.

The receiver employed an array of 12 elements spaced by 12 cm. The receiving array was submerged at the depth of 40 m, while the transmitter depth varied between 40 m and 60 m. The water depth was approximately 100 m, and the transmission distance varied between 3 km and 7 km.

The results presented in this section are based on processing all the 52 rounds of signal recordings, and include four receiver configurations: (1) coherent P-FFT combining alone, (2) coherent P-FFT combining with MP refinement step, (3) coherent P-FFT combining with LS refinement step, and (4) differentially coherent P-FFT combining. The latter two techniques, corresponding to the references [5] and [6], are used as a performance benchmark, as is technique (1) which does not utilize the refinement step.

The overall system performance is evaluated in terms of the average data detection mean squared error (MSE). The per-block MSE is calculated by averaging over all the data carriers,

$$\text{MSE}(K, n) = \frac{1}{K - |\mathcal{K}_p|} \sum_{k \notin \mathcal{K}_p} |\hat{d}_k(n) - d_k(n)|^2 \tag{12}$$

where $n$ is the block number. The overall average is calculated over all the $N_b$ OFDM blocks and all the 52 frames,

$$\text{MSE}(K) = \frac{1}{52 N_b} \sum_n MSE(K, n) \tag{13}$$

Fig. 2 illustrates the scatter plots obtained within one OFDM block with 1024 carriers, 12 receiving elements and 4 partial FFT intervals. The algorithm parameters are listed in Table II.

| $K$ | 128 | 256 | 512 | 1024 | 2048 |
|---|---|---|---|---|---|
| $\alpha$ | 0.1 | 0.3 | 0.45 | 0.55 | 0.65 |
| $\lambda$ | 0.98 | 0.98 | 0.98 | 0.98 | 0.99 |

TABLE II: Algorithm parameters used in coherent P-FFT combining: the RLS forgetting factor $\lambda$ and the channel smoothing parameter $\alpha$ for different number of carriers $K$. MP operates with super-resolution factor $S = 4$ and termination threshold $\eta = -13$ dB.

Fig. 3 summarizes the results of experimental data processing. This figure shows the performance of the four receiver configurations as a function of the number of partial intervals $I$ and the number of carriers $K$. Clearly, MP emerges as the winning technique, but more importantly, we note that partial FFT demodulation in any form offers a viable solution for mobile UWA communications where both high data rate and high quality of performance are required. Even differentially coherent detection provides an impressive $-12$ dB of MSE in configuration with $K = 1024$ carriers and $I = 4$ partial intervals (8.41 kbps in 5 kHz of bandwidth, with pilot overhead taken into account). That performance is matched by coherent P-FFT combining, which alone provides an MSE of $-12$ dB

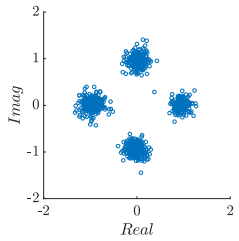


(a) P-FFT differentially coherent combining

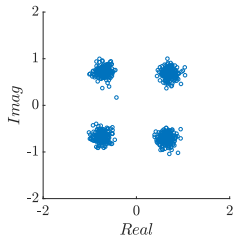


(b) P-FFT coherent combining only.

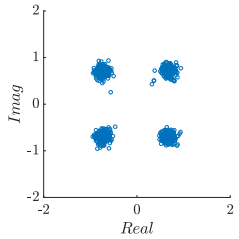


(c) P-FFT coherent combining, LS refinement

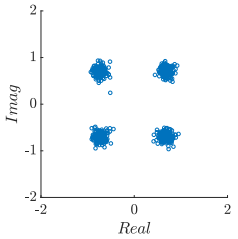


(d) P-FFT coherent combining, MP refinement

Fig. 2: Illustration of the system performance for an OFDM block with $K = 1024$ carriers, $I = 4$ partial intervals, and $M_r = 12$ receiving elements. The average mean squared error calculated over all the data carriers is (a) $-15$ dB, (b) $-16.8$ dB, (c) $-18.7$, and (d) $-19.1$ dB.

of MSE, while the MP refinement offers additional 2 dB of improvement (in contrast, LS offers a negligible improvement). The MP improvement is attributed to the increased resolution ($S = 4$ is used for all the results presented). Regardless of the receiver configuration, performance improves significantly as the number of partial intervals grows from 1 to 8. With $I = 8$ partial intervals, the best performance is achieved with $K = 512$ carriers, but doubling the number of carriers to 1024 incurs a loss of only 1.5 dB. With 2048 carriers the performance deteriorates as the channel coherence time is nudged, although the system stays operational with an MSE on the order of $-10$ dB.

Fig. 4 examines the performance as a function of the number of receiving elements. The $M_r$ receiving elements are chosen from the available 12 elements as maximally spaced. As one might expect, a significant improvement is observed as the number of elements increases and spatial diversity gain is extracted. Although the best performance ($-14$ dB of MSE with MP refinement) is achieved by using all the 12 elements, using just 4 or 6 elements provides an excellent performance as well (the total array aperture remains the same, hence the effect of diminishing returns with increasing $M_r$).

Fig. 5 shows the estimated cumulative density function (CDF) of the MSE per block. The CDF estimate is formed from all the OFDM blocks transmitted over the 3.5 hours. This result refers to $K = 1024$ carriers, $I = 8$ P-FFT intervals, and $M_r = 12$ receiving elements. Differentially coherent combining provides the MSE of $-10$ dB for 90% of the blocks. Similarly, 90% blocks achieve the MSE below $-13$ dB, $-13$ dB and $-15$ dB for P-FFT coherent combining only, P-FFT coherent combining with LS refinement and P-FFT coherent combining with MP refinement, respectively.

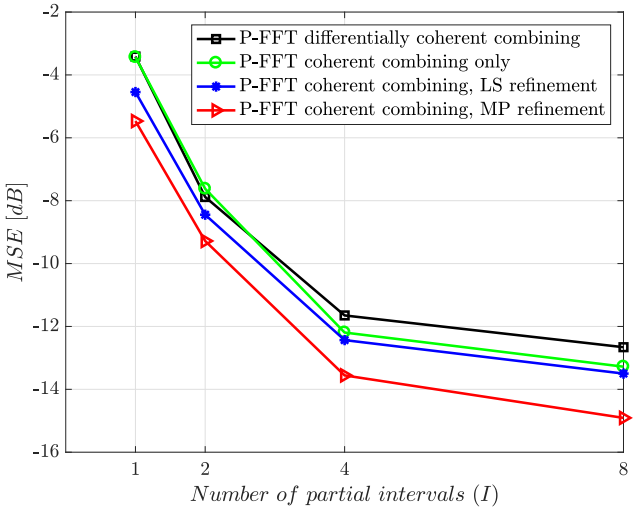


(a) Number of carriers is $K = 1024$.

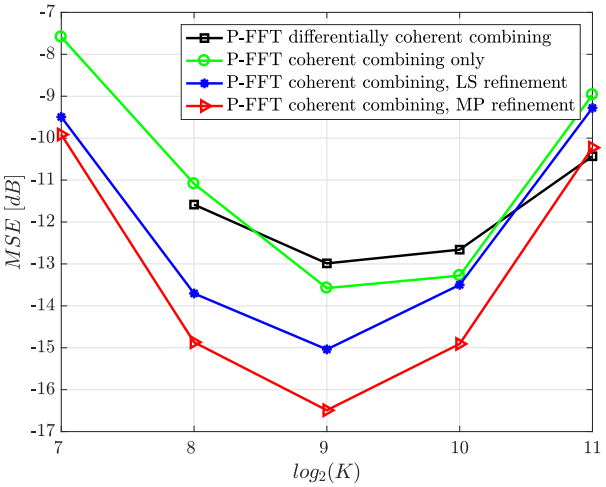


(b) Number of partial FFT intervals is $I = 8$.

Fig. 3: Average mean squared error (MSE) as a function of the number of partial intervals $I$ and the number of carriers $K$ for the four receiver configurations. Both LS and MP channel estimators use tentative decisions from coherent P-FFT combining as pilots. MP operates with super-resolution $S = 4$, and terminates when the absolute ratio of the estimated tap to the strongest tap falls below $-13$ dB. Coherent P-FFT combining operates with $2I$ pilots for initial RLS training, with additional pilots inserted every 8 carriers to avoid error propagation (phase flipping near spectral nulls). Differentially coherent P-FFT combining operates with $2IM_r$ pilots.

Finally, in Fig. 6, we address the performance of the system in which regular low-density parity check (LDPC) codes are

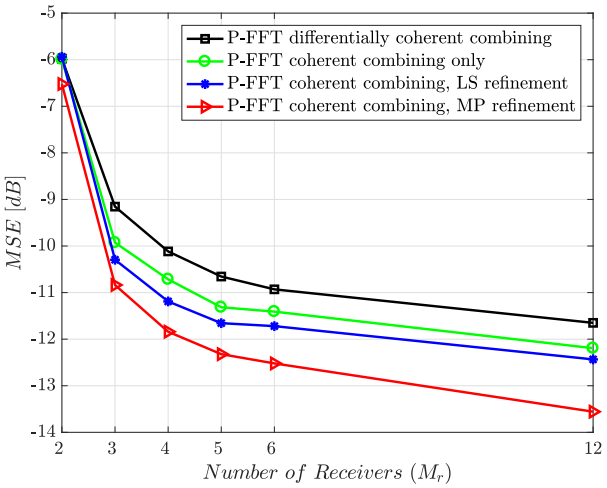


Fig. 4: Average mean squared error (MSE) as a function of the number of receiving elements. The $M_r$ elements are chosen from the available 12 as maximally spaced. The number of carriers is $K = 1024$, and the number of partial intervals is $I = 8$.

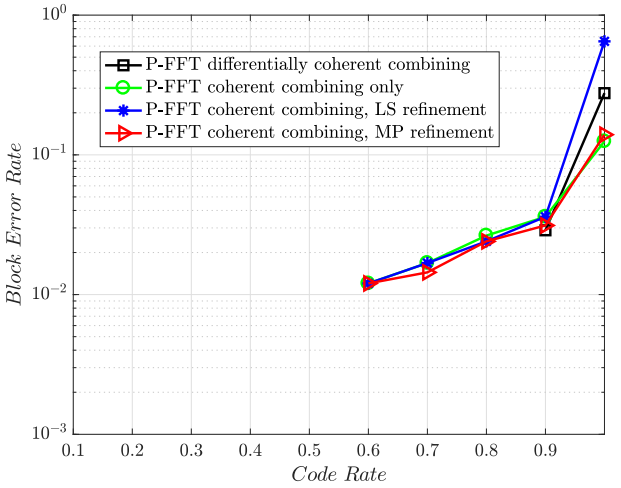


Fig. 6: Block error rate (BLER) measured using the four receiver configurations operating with LDPC codes of varying rate. The number of carriers is $K = 1024$, and the number of partial intervals is $I = 8$. Code rates below 0.6 result in low BLER values that cannot be measured with the existing data.

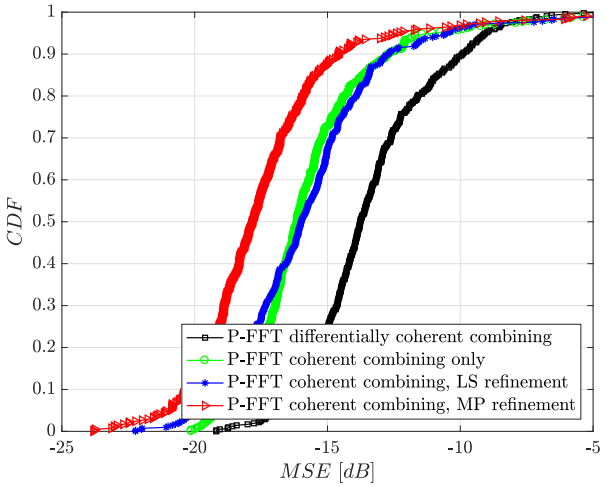


Fig. 5: Empirical cumulative density function (CDF) of the per-block MSE (12). $K = 1024$ carriers, $I = 8$ partial intervals, and $M_r = 12$ array elements are used in this example. Coherent P-FFT combining with MP refinement provides provides MSE below $-15$ dB in about 90% of the OFDM blocks transmitted during the experiment.

used. We consider various code rates ranging from 0.1 to 1, and evaluate the system performance in terms of the average block error rate (BLER). The codeword length is $N = 2K$; thus, each codeword constitutes an OFDM block. The column weight of the $M \times N$ parity check matrix ($M$ is the number of parity bits) is $w_c = 3$ for all the code rates considered, and the row weight $w_r = w_c N/M$, varies from 3.3 to 30 corresponding to the code rates from 0.1 to 0.9 [10]. We use soft decision decoding that takes the likelihood ratio for each code-bit as an input. Decoding is performed based on the probability propagation algorithm which can be seen as an instance of the sum-product algorithm [11]. Employing the P-FFT methods in any form as a pre-FFT ICI mitigation technique enables LDPC to work to its full potential. With code rate as high as 0.8, all the methods achieve the BLER of $2 \times 10^{-2}$. Lower code rates resulted in no errors measurable with the data at hand.

## V. Conclusion

We presented an experimental performance analysis of multichannel partial FFT demodulation of OFDM signals recorded over a mobile acoustic channel. Partial FFT demodulation accounts for pre-FFT compensation of the inter-carrier interference caused by the time variation of the channel, while maximum ratio multichannel combining provides the spatial diversity gain. Four receiver configurations were investigated: coherent P-FFT combining alone, coherent P-FFT combining coupled with least squares or matching pursuit refinement stage, and differentially coherent P-FFT combining. All provided excellent results. Notably, coherent P-FFT combining followed by matching pursuit refinement stage delivered an average MSE below $-15$ dB for 90% of OFDM blocks, and enabled a very high rate LDPC code to achieve an excellent block error rate of $10^{-2}$.

Future research will focus on coupling the P-FFT demodulation with a low-complexity array processing technique to further relieve the computational burden.

## Acknowledgement

This work was supported in part by the following grants: ONR N00014-15-1-2550, NSF 1428567 and CNS-1726512.

## REFERENCES


[1] B. Li, S. Zhou, M. Stojanovic, L. Freitag, and P. Willett, "Multicarrier communication over underwater acoustic channels with nonuniform Doppler shifts," *IEEE J. Ocean. Eng.*, vol. 33, no. 2, pp. 198–209, 2008.

[2] C. R. Berger, S. Zhou, J. C. Preisig, and P. Willett, "Sparse channel estimation for multicarrier underwater acoustic communication: From subspace methods to compressed sensing," *IEEE Trans. Signal Process.*, vol. 58, no. 3, pp. 1708–1721, 2010.

[3] K. Tu, D. Fertonani, T. M. Duman, M. Stojanovic, J. G. Proakis, and P. Hursky, "Mitigation of intercarrier interference for OFDM over time-varying underwater acoustic channels," *IEEE J. Ocean. Eng.*, vol. 36, no. 2, pp. 156–171, 2011.

[4] K. Tu, T. M. Duman, M. Stojanovic, and J. G. Proakis, "Multiple-resampling receiver design for OFDM over Doppler-distorted underwater acoustic channels," *IEEE J. Ocean. Eng.*, vol. 38, no. 2, pp. 333–346, 2013.

[5] S. Yerramalli, M. Stojanovic, and U. Mitra, "Partial FFT demodulation: A detection method for highly doppler distorted OFDM systems," *IEEE Trans. Signal Process.*, vol. 60, no. 11, pp. 5906–5918, 2012.

[6] Y. M. Aval and M. Stojanovic, "Differentially coherent multichannel detection of acoustic OFDM signals," *IEEE J. Ocean. Eng.*, vol. 40, no. 2, pp. 251–268, 2015.

[7] J. Huang, S. Zhou, J. Huang, C. R. Berger, and P. Willett, "Progressive inter-carrier interference equalization for OFDM transmission over time-varying underwater acoustic channels," *IEEE J. Sel. Topics Signal Process.*, vol. 5, no. 8, pp. 1524–1536, 2011.

[8] W. Li and J. C. Preisig, "Estimation of rapidly time-varying sparse channels," *IEEE J. Ocean. Eng.*, vol. 32, no. 4, pp. 927–939, 2007.

[9] A. Tadayon and M. Stojanovic, "Frequency offset compensation for acoustic OFDM systems," in *Proc. IEEE OCEANS'17 Conf.*, Anchorage, AK, 2017, pp. 1–5.

[10] W. Ryan and S. Lin, *Channel codes: classical and modern*. Cambridge University Press, 2009.

[11] D. J. MacKay, "Good error-correcting codes based on very sparse matrices," *IEEE Trans. Inf. Theory*, vol. 45, no. 2, pp. 399–431, 1999.